• Clinical Research •

Comparative diagnostic value of cylindrical dandruff and meibomian gland uneven atrophy for *Demodex* infestation in meibomian gland dysfunction

Ya-Na Fu, Ying Li, Fan Zhang, Shuang-Qing Wu, Lin Liang, Xin-Xin Yu, Zu-Hui Zhang, Xiao-Yu Chen, Qi Dai

National Clinical Research Center for Ocular Diseases, Eye Hospital, Wenzhou Medical University, Wenzhou 325027, Zhejiang Province, China

Co-first Authors: Ya-Na Fu and Ying Li

Correspondence to: Qi Dai. Eye Hospital of Wenzhou Medical University, 270 Xueyuanxi Road, Wenzhou 325027, Zhejiang Province, China. dq@mail.eye.ac.cn

Received: 2025-12-28 Accepted: 2026-05-20

Abstract

• **AIM:** To evaluate the diagnostic utility of meibomian gland uneven atrophy (UA) in identifying *Demodex* infestation among patients with meibomian gland dysfunction (MGD) and to compare its diagnostic performance with that of cylindrical dandruff (CD).

• **METHODS:** Patients with MGD were prospectively enrolled and stratified into four groups (n=25/group) based on the presence/absence of CD and UA. Comparative analyses and multivariate adjustments were performed using *Demodex* detection confirmed by *in vivo* confocal microscopy and light microscopy. Diagnostic performance was evaluated using receiver operating characteristic (ROC) curve analysis.

• **RESULTS:** A total of 100 patients were recruited. The median age was 31.0y (range: 21.0–45.0y; Q1, Q3: 27.0–37.0y), including 29 males and 71 females. *Demodex* counts per eyelash and positivity rates were highest in the CD^+UA^+ group, followed by CD^+UA^-, and CD^-UA^+, and then CD^-UA^-. UA was associated with a 5.521-fold increased likelihood of *Demodex* positivity [95% confidence interval (CI): 2.098–14.531, P=0.001]; CD conferred a 6.460-fold increased risk (95%CI: 2.454–17.002, P<0.001). Incorporating UA status significantly improved model fit ($\Delta\chi^2$=14.096, P<0.001). The areas under the ROC curve (AUC) for CD (in UA^-), UA (in CD^-), and CD+UA (CD^-UA^- and CD^+UA^+) were 0.776, 0.762, and 0.865, respectively. CD and UA demonstrated comparable sensitivity (CD: 87.5%, UA: 86.7%) and specificity (CD: 65.6%, UA: 65.7%), which improved to 90.9% and 82.1%, respectively, when both were combined.

• **CONCLUSION:** UA is a significant predictor of *Demodex* infestation, with diagnostic performance comparable to CD. Combined assessment of CD and UA offers high sensitivity and good specificity, providing a novel and practical tool and substantially reducing misdiagnosis.

• **KEYWORDS:** meibomian gland dysfunction; *Demodex*; ocular demodicosis; cylindrical dandruff; confocal microscopy; eyelid diseases

DOI:10.18240/ijo.2026.10.07

Citation: Fu YN, Li Y, Zhang F, Wu SQ, Liang L, Yu XX, Zhang ZH, Chen XY, Dai Q. Comparative diagnostic value of cylindrical dandruff and meibomian gland uneven atrophy for *Demodex* infestation in meibomian gland dysfunction. *Int J Ophthalmol* 2026;19(10):1939-1947

INTRODUCTION

Demodex mites are the most prevalent ectoparasites inhabiting the human ocular surface, comprising two species: *Demodex folliculorum* (*D.folliculorum*) and *Demodex brevis* (*D.brevis*). The former predominantly colonizes eyelash follicles in clusters, whereas the latter resides deeper within sebaceous glands and meibomian glands (MG)[1]. Pathogenicity arises when mite density exceeds physiological thresholds. Ocular demodicosis exhibits a global prevalence of 14%–89.3%[2], with chronic infestation contributing to progressive MG atrophy and dysfunction[3], dry eye disease (DED), anterior blepharitis, and blepharokeratoconjunctivitis[4-7]. These findings underscore the substantial symptom burden, financial burden, and psychosocial consequences of *Demodex* blepharitis (DB), underscoring the need for effective diagnosis and treatment. The diagnosis of ocular demodicosis typically requires sequential clinical assessment of cylindrical dandruff (CD)—solidified excretions around the base of the eyelash follicles, and direct visualization of mites by light microscopy (LM) or *in vivo* confocal microscopy (IVCM)[8-9]. However, ocular demodicosis is frequently

misdiagnosed or underdiagnosed, particularly in primary care settings. Recently, a multicenter study by seven researchers across six ophthalmology clinics revealed that 44.0% of patients with CD had never been diagnosed with DB[10]. These diagnostic challenges can primarily be attributed to the overlap of symptoms with other ocular surface diseases[11], the lack of microscopic equipment in clinics for mite identification, non-compliance during sampling procedures in pediatric populations, and insufficient clinical experience in identifying CD, particularly atypical or sporadic CD[9]. Failure to diagnose DB can exacerbate disease progression, potentially resulting in severe MG atrophy, refractory DED, chalazion, or corneal inflammation.

With the increasing clinical adoption of meibography, we aimed to identify a more convenient, effective, and simple diagnostic indicator of *Demodex* infestation to alert clinicians and optometrists to the possibility of ocular demodicosis, thereby mitigating diagnostic oversight. Our previous studies used SimCLR neural networks and convolutional neural networks to classify MG images and revealed that uneven dropout patterns of the MG were associated with a higher prevalence of CD positivity and *Demodex* infestation[12-14]. Although the specific pathological mechanism underlying uneven atrophy (UA) induced by *Demodex* mites remains unclear, these findings suggest that UA may function as an adjunctive diagnostic indicator for *Demodex* infestation[14]. The present study was designed to assess the diagnostic utility of UA in detecting *Demodex* infestation and to compare its efficacy with that of CD.

PARTICIPANTS AND METHODS

Ethical Approval This prospective, cross-sectional study was conducted at the Eye Hospital Wenzhou Medical University and received approval from the ethics institutional review board (the approval number: H2023-010-K-07). The study was conducted following the tenets of the Declaration of Helsinki. All patients provided written informed consent. The study was registered in the Chinese Clinical Trial Registry (ChiCTR: www.chictr.org.cn) under identifier: ChiCTR20400081303.

Participants and Subgroups From April 2023 to January 2024, four groups of patients with meibomian gland dysfunction (MGD), visiting the Dry Eye Center of Wenzhou Eye Hospital for the first time (treatment-naïve), were continuously recruited. Three participants who were unable to complete examinations were excluded from analysis. A total of 100 people across the four groups were included in the final analysis. Group allocation (Figure 1A) was based on the presence or absence of UA of the MG in any eyelid of either eye (Figure 1B–1E) and CD at the eyelash base (Figure 1G). Referring to previous research data[13], UA was defined within the central three-quarters of the MG region as follows:

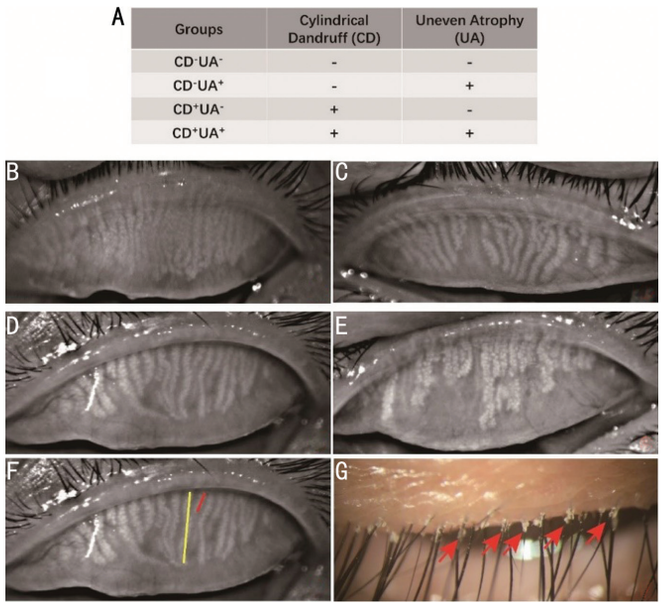

Figure 1 Group assignment by UA and CD status A: Participants were enrolled based on the presence or absence of CD and UA as follows: CD^-, the eyelashes on both upper and lower eyelids are free from debris and CD; visual representation of meibomian gland atrophy; B: Uniform atrophy; C, D, E: UA; F: In the central three-quarters area of the meibomian gland, the height of the shorter gland (marked by the red line, 41.97 pixels) was less than two-thirds the height of the adjacent longer gland (marked by the yellow line, 135.21 pixels). Measurements were performed using ImageJ [http://imagej.nih.gov/ij, Java 1.8.0_112 (64-bit)]. This condition is defined as UA of the meibomian glands; G: Visual representation of CD (red arrows, 25×). CD^+: CD in the eyelashes of at least one upper or lower eyelid; UA^-: The meibomian gland in the upper eyelid of at least one eye exhibits uniform atrophy or is non-atrophic; UA^+: The meibomian gland in the upper eyelid of at least one eye exhibits UA. UA: Uneven atrophy; CD: Cylindrical dandruff.

glandular atrophy was considered uneven when shorter glands measured less than two-thirds the height of adjacent longer glands (Figure 1F). Gland height was defined as the linear distance between the two terminal points of the gland, which typically corresponds to its anatomical length[15]. The presence of UA and CD was determined by two senior ophthalmologists (Fu YN and Dai Q), with any disagreements resolved through consensus with a third specialist (Wu SQ). The exclusion criteria were as follows: patients aged >45y or <18y; those who underwent prior eyelid margin cleaning and *Demodex* treatment with intense pulsed light or terpinen-4-ol therapy before enrolment; those with a history of ocular surgery, trauma, or chemical burns within the past 3mo; those with systemic or local infectious diseases or autoimmune diseases affecting MG function, like rosacea, diabetes, Sjögren's syndrome, or individuals using immunosuppressants; and those with MG atrophy exceeding two-thirds of the total gland area in both eyes.

Ocular Surface Parameters Ocular surface assessments were performed sequentially as follows: Ocular Surface Disease Index (OSDI) questionnaire (score range: 0–100[16], non-invasive tear film breakup time (NIBUT), tear meniscus height (TMH), corneal fluorescein staining (CFS; score range: 0–12)[17], lid margin abnormality (LMA; score range: 0–5)[18], MG expressibility (MGE), meibum quality (MQ), and meibography. LMA, including margin thickening, irregularity of the lid margin, plugging of the gland orifice, vascular engorgement/telangiectasia, and anterior or posterior replacement of the mucocutaneous junction, were scored 0–5. MG expressibility was assessed by applying pressure to five central glands of the lower eyelid and scored on a scale of 0–3[19]. MQ was graded on a scale of 0–3 as follows: grade 0, clear; grade 1, cloudy; grade 2, cloudy with granular debris; and grade 3, thick like toothpaste[19]. The scores from eight MG in the lower eyelid were summed to obtain a total score. NIBUT, TMH, and images of the upper and lower MGs were captured using Keratograph 5M (K5M; Oculus, Wetzlar, Germany). The meiboscore was determined on a scale of 0–3 for each eyelid, and the combined score (range, 0–6) was used for analysis[20].

***Demodex* Examination** Each patient underwent *Demodex* evaluation using both IVCM and LM. The upper eyelid of each eye was scanned using the Heidelberg Retina Tomograph 3 Rostock Cornea Module (Heidelberg Engineering GmbH, Heidelberg, Germany), as previously described, targeting 10 eyelashes and their follicles[21-22]. The images were masked and independently reviewed by two observers (Fu YN and Dai Q). The average number of mites per eyelash was calculated by summing the total number of mites (the average number given by the observers) across the 10 scanned eyelashes. Following IVCM, three eyelashes were epilated from each of the four eyelids exhibiting CD and examined under LM[23]. The total number of *Demodex* mites at all developmental stages across the 12 lashes was recorded. LM-based detection and quantification were performed by a blinded technician. Both IVCM and LM observers were masked to group assignments. *Demodex* positivity was defined as the presence of ≥1 mite per eyelash in any eyelid.

Statistical Analysis Sample size estimation was conducted using PASS 15 (NCSS, Kaysville, UT, USA), based on preliminary IVCM-derived data for average *Demodex* mite count per eyelash. Assuming equal group allocation, α-value of 0.05 (two-sided), and statistical power of 0.8−0.9, the minimum required sample size was 18 participants per group (total n=72). To accommodate an anticipated attrition rate of 20%, the final enrolment target was adjusted to 23 participants per group, yielding a total sample size of 92.

All statistical analyses were conducted using SPSS for Windows (version 19.0; SPSS Inc., Chicago, IL, USA). Continuous variables are presented as mean±standard deviation (for normally distributed data) or median (interquartile range: Q1, Q3; for non-normally distributed data). Categorical variables are reported as numbers (percentages).

Group comparisons were performed using one-way analysis of variance or the Kruskal-Wallis test for multiple independent groups, the Mann-Whitney U test for two independent groups, and the Wilcoxon signed-rank test for paired samples, as appropriate. Categorical variables were compared using Pearson's Chi-square test or McNemar's test. Stratified Chi-square tests were performed to evaluate the incremental predictive value of CD beyond UA, and *vice versa*. Logistic regression models with likelihood ratio tests were employed to quantify the additional diagnostic value contributed by each predictor. Assessment of inter-rater agreement was performed using Cohen's kappa coefficient (κ) for categorical variables and Kendall's tau-b (τ_b) correlation coefficient for non-normally distributed ordinal variables.

The diagnostic performance of CD and UA for detecting *Demodex* infestation was assessed using receiver operating characteristic (ROC) curve analysis. Statistical significance was defined as P<0.05 (or adjusted P<0.05 when pairwise comparisons were corrected with Bonferroni method).

RESULTS

Study Participants A total of 100 patients (25 in each group) were enrolled in this study. The median age was 31.0y (range: 21.0–45.0; Q1, Q3: 27.0–37.0). The cohort comprised 29 male and 71 female participants. No significant differences were observed among the four groups in terms of age, sex ratio, OSDI score, NIBUT, CFS, TMH, MGE, or MQ (Table 1). However, the severity of MG atrophy in the groups with UA (here onwards referred to as UA^+; CD^-UA^+ and CD^+UA^+) was significantly higher than that in the groups without UA (here onwards referred to as UA^-; CD^-UA^- and CD^+UA^-; all adjusted P<0.05; Table 2), whereas no significant differences were identified within the UA^+ groups (CD^-UA^+ *vs* CD^+UA^+, adjusted P=0.999) or within the UA^- groups (CD^-UA^- *vs* CD^+UA^-, adjusted P=0.999). Additionally, LMA were significantly more prevalent in the CD^+UA^+ group than in the CD^-UA^- (adjusted P=0.004) and CD^-UA^+ groups (adjusted P=0.003); no significant differences were observed among the remaining groups (Table 2).

Comparison of *Demodex* Infestation in Groups Defined by CD and/or UA Across all 100 patients, the average mite count/lash of both eyes measured by IVCM tended to be higher than that derived from LM [IVCM: 0.86 (Q1, Q3: 0.50–1.54) *vs* LM: 0.08 (Q1, Q3: 0.00–0.31); P<0.001, Wilcoxon test]. A similar trend was observed in *Demodex* positivity rates (IVCM: 49/100 *vs* LM: 22/100; P<0.001, McNemar test).

Table 1 Descriptive demographic data and clinical features of study participants *n* (%), mean±SD, or median (Q1, Q3)

Parameters	Group (overall *n*=100)				$F/H/\chi^2$	*P*
	CD^-UA^- group (*n*=25)	CD^-UA^+ group (*n*=25)	CD^+UA^- group (*n*=25)	CD^+UA^+ group (*n*=25)		
Age (y)	30.72±5.10	33.36±6.22	31.56±6.90	32.48±6.38	0.851	0.469[a]
Female	18 (72)	17 (68)	18 (72)	18 (72)	0.146	0.986[c]
OSDI (scores)	35.48±19.86	34.46±15.89	33.51±19.78	31.87±13.75	0.189	0.904[a]
NIBUT (s)	4.83 (3.94, 8.08)	5.78 (4.13, 8.82)	4.69 (3.87, 7.79)	5.45 (3.69, 6.69)	3.642	0.303[b]
CFS (scores)	0 (0, 1.50)	0 (0, 1.88)	0 (0, 0.25)	0 (0, 1.50)	0.897	0.826[b]
TMH (mm)	0.26±0.08	0.22±0.08	0.22±0.06	0.25±0.08	2.233	0.089[a]
LMA (scores)	2.00 (0.50, 2.00)	1.00 (1.00, 2.00)	2.00 (1.00, 3.00)	3.00 (2.00, 4.00)	16.603	0.001[b]
MGE (scores)	1.00 (0, 1.50)	1.00 (0.25, 2.00)	1.00 (0, 1.38)	1.00 (1.00,1.75)	1.736	0.629[b]
MQ (scores)	15.62±8.08	18.28±7.23	16.52±8.42	18.98±7.11	1.002	0.395[a]
Meiboscore (scores)	1.00 (0.50, 2.00)	3.50 (2.50, 4.00)	1.50 (1.00, 2.25)	2.50 (2.00, 3.75)	36.174	<0.001[b]

[a]ANOVA test; [b]Kruskal-Wallis test; [c]Pearson's Chi-square test. OSDI: Ocular Surface Disease Index; NIBUT: Non-invasive tear film breakup time; CFS: Corneal fluorescein staining; LMA: Lid margin abnormalities; TMH: Tear meniscus height; MGE: Meibomian gland expressibility; MQ: Meibum quality; SD: Standard deviation; Q1: The first quartile; Q3: The third quartile; ANOVA: Analysis of variance.

Table 2 Paired comparison of LMA scores and meiboscore

Paired groups	LMA scores			Meiboscore		
	Z	*P*	Adjusted *P*	*Z*	*P*	Adjusted *P*
CD^-UA^- *vs* CD^-UA^+	0.920	0.908	0.999	-42.100	<0.001	<0.001
CD^-UA^- *vs* CD^+UA^-	-14.320	0.072	0.429	-10.780	0.185	0.999
CD^-UA^- *vs* CD^+UA^+	-26.920	0.001	0.004	-35.600	<0.001	<0.001
CD^-UA^+ *vs* CD^+UA^-	-15.240	0.055	0.331	31.320	<0.001	0.001
CD^-UA^+ *vs* CD^+UA^+	-27.840	<0.001	0.003	6.500	0.425	0.999
CD^+UA^- *vs* CD^+UA^+	-12.600	0.113	0.677	-24.820	0.002	0.014

Pairwise comparisons using Mann-Whitney *U* test with Bonferroni correction; statistical significance was defined as adjusted *P*<0.05. Negative *Z* values reflect directional ranking differences. LMA and Meiboscore are non-parametric variables. LMA, including margin thickening, irregularity of the lid margin, plugging of the gland orifice, vascular engorgement/telangiectasia, and anterior or posterior replacement of the mucocutaneous junction, were scored from 0–5. The meiboscore was determined on a scale from 0–3 for each eyelid, and the combined score (range, 0–6) was used for analysis. LMA: Lid margin abnormalities; UA: Uneven atrophy; CD: Cylindrical dandruff.

Table 3 presents *Demodex* infestation data across the four groups based on LM and IVCM. LM-based analysis revealed no significant differences in average mite count per eyelash or *Demodex* positivity rate among the four groups. Similarly, no significant differences were observed in either measure when comparing UA^+ and UA^- participants (average mite count/lash: *P*=0.139, Mann-Whitney *U* test; *Demodex* positivity rate: *P*=0.629, Pearson's Chi-square test). However, CD^+ individuals had a significantly higher average mite count/lash than CD^- individuals [CD^+: 0.17 (Q1, Q3: 0.00–0.33) *vs* CD^-: 0.08 (Q1, Q3: 0.00–0.19); *P*=0.024, Mann-Whitney *U* test], whereas the *Demodex* positivity rate did not differ significantly between the two groups (*P*=0.053, Pearson's Chi-square test).

Interestingly, IVCM results showed that both the average mite count/lash and the *Demodex* positivity rate differed significantly among the four groups, with the highest in the CD^+UA^+ group, followed by the CD^+UA^-, CD^-UA^+, and then CD^-UA^- groups (Table 3). The CD^-UA^- group had both the minimal average mite count/lash (all adjusted *P*<0.05) and the lowest *Demodex* positivity rate (all adjusted *P*<0.05; Table 4). However, no significant differences were found in either average mite count/lash or *Demodex* positivity rate among the CD^+UA^+, CD^+UA^-, and CD^-UA^+ groups (Table 4).

Difference of *Demodex* Infestation After Adjustment for CD or UA Among all 100 participants, differences in *Demodex* infestation measured by IVCM, after adjusting for CD or UA, are summarized in Table 5. After adjusting for CD status, we found that the UA^+ group had higher average mite counts per lash than the UA^- group in both CD^- (*P*<0.001) and CD^+ subcategories (*P*=0.041). A similar trend was obtained for *Demodex* positivity rates. UA^+ participants had a 5.521-fold higher risk of *Demodex* positivity than UA^- participants [adjusted odds ratio (OR)=5.521, 95% confidence interval (CI): 2.098–14.531, *P*=0.001]. The Breslow-Day test for homogeneity of OR (χ^2=1.752, *P*=0.186) suggested no significant variation in the *Demodex* detection across CD strata. Stratified analyses (adjusted for CD status) revealed a stronger association between UA and *Demodex* infestation

Table 3 *Demodex* mite evaluation by LM and IVCM *n* (%) or median (Q1, Q3)

Parameters	Group (overall *n*=100)				H/χ^2	*P*
	CD^-UA^- (*n*=25)	CD^-UA^+ (*n*=25)	CD^+UA^- (*n*=25)	CD^+UA^+ (*n*=25)		
LM						
Positive rate	3 (12)	4 (16)	7 (28)	8 (32)	3.963	0.266[c]
OU upper and lower lid						
Mite count/lash	0 (0, 0.13)	0.08 (0, 0.25)	0.08 (0, 0.33)	0.17 (0.08, 0.38)	7.295	0.063[b]
IVCM						
Positive rate	2 (8)	13 (52)	14 (56)	20 (80)	27.011	<0.001[c]
OU upper lid						
Mite count/lash	0.45 (0.18, 0.78)	0.95 (0.55, 1.63)	1.10 (0.45, 1.68)	1.40 (0.83, 1.90)	28.730	<0.001[b]

Demodex positivity status: ≥1 mite per lash in any eyelid; [b]Kruskal-Wallis test; [c]Pearson's Chi-square test. LM: Light microscope; IVCM: *In vivo* confocal microscopy; UA: Uneven atrophy; CD: Cylindrical dandruff; OU: *Oculus uterque*; Q1: The first quartile; Q3: The third quartile.

Table 4 Paired comparison of mean mites or positivity rate measured by IVCM

Paired groups	Mean mites per lash			Positivity rate		
	Z	*P*	Adjusted *P*[a]	χ^2	*P*	Adjusted *P*[b]
CD^-UA^- *vs* CD^-UA^+	-29.460	<0.001	0.002	11.524	0.001	0.006
CD^-UA^- *vs* CD^+UA^-	-26.180	0.002	0.008	13.235	<0.001	0.002
CD^-UA^- *vs* CD^+UA^+	-43.240	<0.001	<0.001	26.299	<0.001	<0.001
CD^-UA^+ *vs* CD^+UA^-	3.280	0.680	0.999	0.081	0.777	0.999
CD^-UA^+ *vs* CD^+UA^+	-13.780	0.092	0.558	4.367	0.037	0.222
CD^+UA^- *vs* CD^+UA^+	-17.060	0.036	0.225	3.309	0.069	0.414

[a]Pairwise comparisons using Mann-Whitney *U* test with Bonferroni correction, statistical significance was defined as adjusted *P*<0.05. [b]Post hoc pairwise Chi-square tests with Bonferroni correction, statistical significance was defined as adjusted *P*<0.05. IVCM: *In vivo* confocal microscopy; UA: Uneven atrophy; CD: Cylindrical dandruff.

in the CD^- group (OR=12.458, 95%CI: 2.407–64.495) than in the CD^+ group (OR=3.143, 95%CI: 0.893–11.064). In the UA-adjusted analysis, CD^+ individuals had higher average mite count/lash than CD^- individuals in both UA^- (*P*=0.001) and UA^+ categories (*P*=0.053). Additionally, CD^+ individuals had a 6.460 times higher risk of *Demodex* positivity than CD^- individuals (adjusted OR=6.460, 95%CI: 2.454–17.002, *P*<0.001). The Breslow-Day test for homogeneity of OR (χ^2=1.750, *P*=0.186) demonstrated consistency in the association between CD and *Demodex* detection across UA strata. Stratified analysis (adjusted for UA) also indicated that the association between CD and *Demodex* infestation was stronger in the UA^- group (OR=14.636, 95%CI: 2.820–75.954) than in the UA^+ group (OR=3.692, 95%CI: 1.052–12.957; Table 5). These findings indicate that both UA and CD are independently associated with *Demodex* infestation, regardless of the presence of the other.

Univariate logistic regression analysis revealed that both CD (likelihood ratio χ^2=122.773; *P*<0.001) and UA (likelihood ratio χ^2=126.790; *P*=0.001) were significantly associated with increased *Demodex* positivity. Incorporating UA status into the CD-based model significantly improved model fit [likelihood ratio test: $\Delta\chi^2$=14.096, degree of freedom (df)=1, *P*<0.001], demonstrating that UA provides independent explanatory value for mite detection and contributes more substantially than CD alone. Similarly, adding CD to the UA-based model also enhanced model fit (likelihood ratio test: $\Delta\chi^2$=17.114, *df*=1; *P*<0.001). These findings indicate that CD and UA enhance each other's ability to predict the risk of *Demodex* infestation.

Diagnostic Performance of UA or CD Characteristics The low detection rate and absence of intergroup differences demonstrated the inadequate sensitivity of LM for *Demodex* detection, supporting the use of IVCM as a superior diagnostic standard. Therefore, we evaluated the diagnostic validity of CD, UA, and the combination of CD+UA in screening *Demodex* infestation based on the *Demodex* positivity results from IVCM. To eliminate the mutual interference between CD and UA, we constructed ROC curves separately: CD was assessed in UA^- groups (CD^-UA^- and CD^+UA^-), UA was assessed in the CD^- groups (CD^-UA^- and CD^-UA^+), and CD+UA were assessed in the CD^-UA^- and CD^+UA^+ groups. The AUC values for UA, CD, and CD+UA were 0.762 (95%CI: 0.621–0.903, *P*=0.004), 0.776 (95%CI: 0.639–0.912, *P*=0.002), and 0.865 (95%CI: 0.756–0.975, *P*<0.001), respectively (Figure 2). The sensitivity values of CD, UA, and CD+UA were 87.5%, 86.7%, and 90.9%, respectively, whereas the specificities were 65.6%, 65.7%, and 82.1%, respectively.

Table 5 Comparison of *Demodex* infestation after adjustment for CD/UA based on IVCM results

Study participants	Subgroups	Mean mite count/lash[a]			*Demodex* positivity rate[b]			
		Median (Q1, Q3)	*U*	*P*	*n* (%)	χ^2	*P* (χ^2)	OR (95%CI)
Total	UA$^-$	0.55 (0.29, 1.16)	668.500	<0.001	16 (32)	11.565	0.001	4.125 (1.792–9.697)[c]
	UA$^+$	1.25 (0.70, 1.76)			33 (66)			
CD$^-$	UA$^-$	0.45 (0.18, 0.78)	118.000	<0.001	2 (8)	11.524	0.001	12.458 (2.407–64.495)
	UA$^+$	0.95 (0.55,1.63)			13 (52)			
CD$^+$	UA$^-$	1.10 (0.45, 1.68)	207.000	0.041	14 (56)	11.565	0.069	3.143 (0.893–11.064)
	UA$^+$	1.40 (0.83, 1.90)			20 (80)			
Total	CD$^-$	0.65 (0.38, 1.04)	750.500	0.001	15 (30)	14.446	<0.001	4.958 (2.124–11.576)[d]
	CD$^+$	1.23 (0.62, 1.76)			34 (68)			
UA$^-$	CD$^-$	0.45 (0.18,0.78)	147.000	0.001	2 (8)	13.235	<0.001	14.636 (2.820–75.954)
	CD$^+$	1.10 (0.45,1.68)			14 (56)			
UA$^+$	CD$^-$	0.95 (0.55,1.63)	213.000	0.053	13 (52)	4.367	0.037	3.692 (1.052–12.957)
	CD$^+$	1.40 (0.83,1.90)			20 (80)			

[a]Mann-Whitney *U* test; [b]Cochran-Mantel-Haenszel test; [c]Breslow-Day test: χ^2=1.752, *P*=0.186; Mantel-Haenszel test: χ^2=11.734, *P*=0.001; adjusted OR (95%CI)=5.521 (2.098–14.531), *P*=0.001; [d]Breslow-Day test: χ^2=1.750, *P*=0.186; Mantel-Haenszel test: χ^2=14.367, *P*<0.001; adjusted OR (95%CI)=6.460 (2.454-17.002), *P*<0.001. UA: Uneven atrophy; CD: Cylindrical dandruff; Q1: The first quartile; Q3: The third quartile; CI: Confidence interval; OR: Odds ratio; IVCM: *In vivo* confocal microscopy.

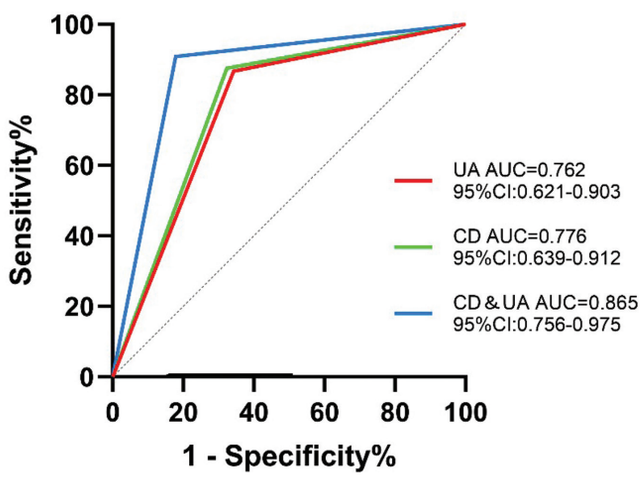

Figure 2 ROC curves of UA, CD, and their combined effect either in the specific population UA: Uneven atrophy; CD: Cylindrical dandruff; ROC: Receiver operating characteristic curve; AUC: Areas under the ROC curve; CI: Confidence interval.

The Youden's index values were calculated as 0.55, 0.53, and 0.63, respectively.

Evaluation of Inter-Rater Agreement The presence of UA and CD was determined by two assessors, who were blind to both each other's evaluation and group assignments. Agreement of the two assessors was substantial for UA (Cohen's κ=0.82, *P*<0.001) and almost perfect for CD (Cohen's κ=0.90, *P*<0.001). Detection images were masked and independently reviewed by two observers as well. Also, excellent interobserver agreement was demonstrated for IVCM quantification of *Demodex* mites in both eyes (Kendall's τ_b=0.91, *P*<0.001), indicating high diagnostic consistency.

DISCUSSION

Herein, we evaluated the diagnostic utility of UA of the MGs for identifying *Demodex* infestation in MGD, compared its performance with the conventional indicator CD, and determined whether a combined CD and UA approach improves diagnostic accuracy. Our key findings demonstrated that UA was an independent predictor of *Demodex* infestation, with diagnostic performance comparable to that of CD. The combination of CD and UA further elevated diagnostic sensitivity and specificity, providing a practical supplementary approach to reduce underdiagnosis of *Demodex*-related MGD in clinical settings.

Demodex mites are common ectoparasites closely associated with MGD and chronic blepharitis. Previous studies have reported significantly higher *Demodex* infestation rates in patients with MGD (57.14%–89.32%) than healthy controls (1.4%–34%)[24-28]. Mite colonization leads to persistent inflammation, MG duct obstruction, hyperkeratinization, and progressive structural damage, all of which contribute to the development and exacerbation of MGD[29]. CD, characterized by cuff-like debris at the base of eyelashes, has long been recognized as a classic clinical sign of *Demodex* infestation[9,30]. However, reliance on CD alone leads to frequent underdiagnosis, especially in patients without obvious CD but with substantial mite load. In our cohort, 15 of 50 CD-negative patients were confirmed *Demodex*-positive by IVCM, highlighting the risk of missed diagnosis. In this study, we identified that UA, easily observed during routine meibography, serves as a reliable supplementary indicator for *Demodex* infestation.

ROC analysis demonstrated that both CD and UA exhibited comparably high sensitivity (CD: 87.5%; UA: 86.7%), yet relatively low specificity (CD: 65.6%; UA: 65.7%). When combined, CD and UA yielded excellent sensitivity (90.9%) and improved specificity (82.1%). The combined diagnostic model achieved an AUC of 0.865, substantially higher than that of CD (AUC: 0.776) or UA (AUC: 0.762) alone. UA demonstrated equivalent diagnostic value to CD and should be considered accordingly in clinical practice.

Importantly, CD and UA differ in their clinical implications for *Demodex* evaluation. Due to the progressive deterioration of MG caused by *Demodex* mites, CD generally manifests in the early stages of infestation. Specifically, CD exclusively reflects the current activity of *Demodex* mites within eyelash follicles, without capturing mite activity in MGs. In contrast, UA may represent cumulative glandular damage resulting from ongoing or past infestations of *D.folliculorum* and *D.brevis*. This impairment usually requires long time to become apparent. Previous studies have confirmed that *Demodex* mites induce MG UA through multiple pathological pathways. First, *Demodex* brevis resides in MG ducts and causes direct mechanical obstruction, leading to focal meibum stasis, ductal dilation, and localized acinar atrophy[31-34]. Second, mites trigger chronic inflammatory and immune responses, releasing proinflammatory cytokines[35] that aggravate focal gland injury. Third, *Demodex* infestation promotes ductal hyperkeratinization, increased meibum viscosity, and recurrent chalazion formation[36], all contributing to uneven, focal MG damage. Moreover, the gregarious distribution of *Demodex* mites results in inconsistent parasitic load across the tarsus, directly accounting for the spatially heterogeneous pattern of MG atrophy. Collectively, these pathological changes produce the typical UA pattern, which serves as a directly observable morphological sign for identifying suspected *Demodex* infestation during routine meibography. The observed UA likely stems from asymmetric parasitic load distribution—where variations in mite population density across different eyelash follicles or MG create focal atrophic changes. Comparative quantification of mite infestation density across MG regions exhibiting varying degrees of atrophy may serve as a valuable strategy for further hypothesis validation.

Although *Demodex* infestation contributes to the development of MGD and blepharitis, *Demodex* mites can also colonize healthy individuals as subclinical infestation[37]. The specific pathogenic mechanism of *Demodex* mites may be related to mite load, as healthy individuals typically exhibit low parasitic density without obvious glandular damage, whereas symptomatic patients often present with significantly elevated mite counts. Epidemiological studies have reported *Demodex* prevalence of 12.0% in healthy children[38] and 13.3% in the general adult population[37], with *D.folliculorum* accounting for the majority of cases. In addition, *Demodex* species may be another key factor underlying the distinct pathogenicity observed. The two species differ in colonization sites: *D.folliculorum* inhabits eyelash follicles, whereas *D.brevis* resides in MG leading to lower detectability by conventional methods. Notably, our study did not differentiate between these two *Demodex* species, as IVCM has high sensitivity but cannot reliably distinguish between species, while LM allows species identification but exhibits low detection sensitivity, making reliable species-specific stratification unfeasible. Recent research has begun exploring the genomic characteristics of *D.folliculorum* and *D.brevis* from a genetic perspective. These studies have identified variations in 30 genes related to metabolic processes, motility, detoxification, stress response, and allergic reactions[39]. Such genetic divergence may underlie the distinct pathogenic mechanisms observed between the two mite species. These findings offer promising insights for mite detection and pathological research. In the future, integrating optimized mite detection methods, biochemical signatures, and morphological characteristics of MG atrophy could enhance clinicians' understanding of pathogenic mechanisms and therapeutic strategies.

No universally accepted criteria exist for defining *Demodex* positivity, primarily due to methodological variability. IVCM and LM are internationally recognized modalities for ocular *Demodex* detection. Given that *Demodex* mites may be present in asymptomatic individuals[40], *Demodex* positive in this study was defined as ≥1 mite per eyelash detected by IVCM or ≥3 mites across 3 lashes in any eyelid examined by LM[21,32,41]. IVCM demonstrated significantly greater sensitivity than LM for detecting *Demodex* mites across all subjects, consistent with prior research[9,41-42]. IVCM identified significantly higher positivity rates and mite counts in individuals with UA or CD fragments than non-carriers (both $P<0.05$), whereas LM showed no significant differences ($P=0.629$). Therefore, IVCM results were adopted as the definitive diagnostic standard for *Demodex* infestation. These findings highlight the importance of standardizing diagnostic methodology. However, in China and many other developing regions, LM remains the primary diagnostic tool due to limited access to IVCM. This presents a diagnostic challenge for ocular demodicosis. UA may serve as a valuable adjunctive marker to reduce missed diagnoses in settings lacking advanced imaging equipment.

To the best of our knowledge, this is the first study to compare the diagnostic value of UA and CD for *Demodex* infestation. However, this study has several limitations. First, the study population exclusively comprised MGD patients with no healthy controls. The absence of healthy controls limits the evaluation of UA specificity in the general population.

Second, UA is a qualitative indicator proposed by our previous research based on the total variation principle[13], which suggested a cutoff of approximately one-third reduction in the height of adjacent MGs for distinguishing DB from MGD. Meanwhile, analyzing *Demodex* density and UA correlation necessitates a robust quantitative framework. Our prior studies developed multiple MG atrophy indices, total variation-based unevenness, energy curves, cross-entropy, average deviation, shape matching, and entropy-based tortuosity[13,43-44], yet all exhibit inherent constraints: segmentation artifacts impair total variation metrics; gland density biases energy/entropy measures; curve extraction accuracy dictates shape/tortuosity assessments; crucially, no existing parameter holistically captures *Demodex*-driven atrophy complexity. Thus, the definition of UA requires further refinement through large-scale studies to optimize its diagnostic performance. Third, all data were derived from the Han Chinese population in China, raising questions about whether UA and its combination with CD will perform similarly in other ethnic groups or geographic regions. Future work should include multiethnic cohorts to validate these findings.

In conclusion, UA is a robust, easily observable marker that can be readily assessed during routine meibography, expanding diagnostic options to improve detection of *Demodex*-associated disease.

ACKNOWLEDGEMENTS

We sincerely acknowledge Dr. Fen-Fen Li and Mr. Liu-Hong Tian for their statistical expertise in study design. We also would like to express gratitude to the participants involved in this study and to the staff who contribute their efforts.

Authors' Contributions: Fu YN: Conceptualization, funding acquisition, formal analysis, investigation, methodology, project administration, resources, supervision, visualization, writing–original draft, writing–review & editing. Li Y: Data curation, formal analysis, investigation, resources, visualization, writing–original draft, writing–review & editing. Zhang F: Investigation, validation, visualization, writing–original draft. Wu SQ: Investigation, resources, validation. Liang L: Investigation, resources, data curation. Yu XX: Investigation, resources. Zhang ZH: Investigation, resources. Chen XY: Investigation, data curation. Dai Q: Conceptualization, funding acquisition, investigation, resources, methodology, project administration, supervision, writing–review & editing.

Data Availability Statement: The datasets generated and/or analyzed in the current study are available from the corresponding author upon reasonable request.

AI-Generated Content Disclosure: The authors declare that no artificial intelligence generated content was used in this work.

Foundations: Supported by the Wenzhou Municipal Science and Technology Bureau (No.Y2023814); Joint TCM Science & Technology Projects of National Demonstration Zones for Comprehensive TCM Reform (No.GZY-ZJ-KJ-23086).

Conflicts of Interest: Fu YN, None; **Li Y,** None; **Zhang F,** None; **Wu SQ,** None; **Liang L,** None; **Yu XX,** None; **Zhang ZH,** None; **Chen XY,** None; **Dai Q,** None.

REFERENCES

1 Zhang AC, Muntz A, Wang MTM, *et al*. Ocular *Demodex*: a systematic review of the clinical literature. *Ophthalmic Physiologic Optic* 2020;40(4):389-432.

2 Bitton E, Aumond S. *Demodex* and eye disease. *Clin Exp Optom* 2021;104(3):285-294.

3 Ding SC, Zhan Q, Wang JM, *et al*. Factors affecting meibomian gland area loss in symptomatic adults. *Int J Ophthalmol* 2024;17(6):1036-1041.

4 Koo H, Kim TH, Kim KW, *et al*. Ocular surface discomfort and *Demodex*: effect of tea tree oil eyelid scrub in *Demodex* blepharitis. *J Korean Med Sci* 2012;27(12):1574.

5 Zhao YE, Wu LP, Hu L, *et al*. Association of blepharitis with *Demodex*: a meta-analysis. *Ophthalmic Epidemiol* 2012;19(2):95-102.

6 Ben Hadj Salah W, Baudouin C, Doan S, *et al*. *Demodex* and ocular surface disease. *J Fr Ophtalmol* 2020;43(10):1069-1077.

7 Li X, Hou P, Qi XL, *et al*. Clinical manifestation and management of severe blepharokeratoconjunctivitis combined with corneal perforation. *Int J Ophthalmol* 2025;18(2):229-236.

8 Rhee MK, Yeu E, Barnett M, *et al*. *Demodex* blepharitis: a comprehensive review of the disease, current management, and emerging therapies. *Eye Contact Lens* 2023;49(8):311-318.

9 Gao YY, Di Pascuale MA, Li W, *et al*. High prevalence of *Demodex*in eyelashes with cylindrical dandruff. *Invest Ophthalmol Vis Sci* 2005;46(9):3089-3094.

10 Trattler W, Karpecki P, Rapoport Y, *et al*. The prevalence of *Demodex* blepharitis in US eye care clinic patients as determined by collarettes: a pathognomonic sign. *Clin Ophthalmol* 2022;16:1153-1164.

11 Luo XH, Li J, Chen C, *et al*. Ocular demodicosis as a potential cause of ocular surface inflammation. *Cornea* 2017;36 Suppl 1(Suppl 1): S9-S14.

12 Li SY, Wang YY, Yu CY, *et al*. Unsupervised learning based on meibography enables subtyping of dry eye disease and reveals ocular surface features. *Invest Ophthalmol Vis Sci* 2023;64(13):43.

13 Liu XY, Fu YN, Wang DD, *et al*. Uneven index: a digital biomarker to prompt demodex blepharitis based on deep learning. *Front Physiol* 2022;13:934821.

14 Yu XX, Fu YN, Lian HL, *et al*. Uneven meibomian gland dropout in patients with meibomian gland dysfunction and demodex infestation. *J Clin Med* 2022;11(17):5085.

15 Lin XL, Fu YN, Li L, *et al*. A novel quantitative index of meibomian gland dysfunction, the meibomian gland tortuosity. *Trans Vis Sci Tech* 2020;9(9):34.

16 Asiedu K, Kyei S, Mensah SN, *et al*. Ocular surface disease index

(OSDI) versus the standard patient evaluation of eye dryness (SPEED): a study of a nonclinical sample. *Cornea* 2016;35(2):175-180.

17 Song XJ, Zhao P, Wang GY, *et al*. The effects of estrogen and androgen on tear secretion and matrix metalloproteinase-2 expression in lacrimal glands of ovariectomized rats. *Invest Ophthalmol Vis Sci* 2014;55(2):745-751.

18 Foulks GN, Bron AJ. Meibomian gland dysfunction: a clinical scheme for description, diagnosis, classification, and grading. *Ocul Surf* 2003;1(3):107-126.

19 Lee H, Min K, Kim EK, *et al*. Minocycline controls clinical outcomes and inflammatory cytokines in moderate and severe meibomian gland dysfunction. *Am J Ophthalmol* 2012;154(6):949-957.e1.

20 Arita R, Itoh K, Inoue K, *et al*. Noncontact infrared meibography to document age-related changes of the meibomian glands in a normal population. *Ophthalmology* 2008;115(5):911-915.

21 Wang YJ, Ke M, Chen XM. Prospective study of the diagnostic accuracy of the *in vivo* laser scanning confocal microscopy for ocular demodicosis. *Am J Ophthalmol* 2019;203:46-52.

22 Yan T, Dai Q, Yu G. *In vivo* confocal microscopy: a standard operating procedure for the detection of demodex mites at the eyelid margin. *J Vis Exp* 2025;(221).

23 Liang LY, Ding XH, Tseng SCG. High prevalence of demodex brevis infestation in chalazia. *Am J Ophthalmol* 2014;157(2):342-348.e1.

24 Venecia AB, Siong RL. *Demodex* sp. infestation in anterior blepharitis, meibomian-gland dysfunction, and mixed blepharitis. *Philipp J Ophthalmol* 2011, 36(1):15-22.

25 Bhandari V, Reddy JK. Blepharitis: always remember demodex. *Middle East Afr J Ophthalmol* 2014;21(4):317-320.

26 Ding G, Tan Y, Zhang CM, *et al*. Analysis of *Demodex* infection rate and risk factors in patients with meibomian gland dysfunction. *Int Ophthalmol* 2023;43(3):877-884.

27 Hao YR, Zhang XY, Bao JY, *et al*. *Demodex* folliculorum infestation in meibomian gland dysfunction related dry eye patients. *Front Med* 2022;9:833778.

28 Vargas-Arzola J, Segura-Salvador A, Torres-Aguilar H, *et al*. Prevalence and risk factors to *Demodex* folliculorum infection in eyelash follicles from a university population of Mexico. *Acta Microbiol Immunol Hung* 2020;67(3):156-160.

29 Cheng SN, Zhang MC, Chen H, *et al*. The correlation between the microstructure of meibomian glands and ocular *Demodex* infestation: a retrospective case-control study in a Chinese population. *Medicine* 2019;98(19):e15595.

30 Kheirkhah A, Blanco G, Casas V, *et al*. Fluorescein dye improves microscopic evaluation and counting of demodex in blepharitis with cylindrical dandruff. *Cornea* 2007;26(6):697-700.

31 Gutgesell VJ, Stern GA, Hood CI. Histopathology of meibomian gland dysfunction. *Am J Ophthalmol* 1982;94(3):383-387.

32 Sun XW, Liu ZL, Sun SS, *et al*. The correlation between *Demodex* infestation and meibomian gland dysfunction at different ages. *BMC Ophthalmol* 2022;22(1):388.

33 Lee WJ, Kim M, Lee SH, *et al*. The varied influence of ocular *Demodex* infestation on dry eye disease and meibomian gland dysfunction across different age groups. *Sci Rep* 2023;13:16324.

34 Mizuno M, Kawashima M, Uchino M, *et al*. *Demodex*-mite infestation in cilia and its association with ocular surface parameters in Japanese volunteers. *Eye Contact Lens* 2020;46(5):291-296.

35 Kim JT, Lee SH, Chun YS, *et al*. Tear cytokines and chemokines in patients with *Demodex* blepharitis. *Cytokine* 2011;53(1):94-99.

36 Akkucuk S, Kaya OM, Aslan L, *et al*. Prevalence of *Demodex* folliculorum and *Demodex* brevis in patients with blepharitis and chalazion. *Int Ophthalmol* 2023;43(4):1249-1259.

37 Gutiérrez B, Soto R, Catalán A, *et al*. *Demodex folliculorum* (Trombidiformes: Demodicidae) and *Demodex brevis* prevalence in an extreme environment of Chile. *J Med Entomol* 2021;58(6):2067-2074.

38 Zhang N, Liu Y, Wen KY, *et al*. Prevalence of ocular demodex infestation in children: an epidemiological survey in South China. *Eye Contact Lens Sci Clin Pract* 2021;47(1):60-64.

39 Hu L, Zhao YE, Niu DL, *et al*. *De novo* transcriptome sequencing and differential gene expression analysis of two parasitic human *Demodex* species. *Parasitol Res* 2019;118(12):3223-3235.

40 Kosik-Bogacka DI, Łanocha N, Łanocha A, *et al*. *Demodex folliculorum* and *Demodex brevis* in healthy and immunocompromised patients. *Ophthalmic Epidemiol* 2013;20(3):159-163.

41 Arici C, Mergen B, Bahar Tokman H, *et al*. Investigation of the *Demodex* lid infestation with *in vivo* confocal microscopy versus light microscopy in patients with seborrheic blepharitis. *Ocul Immunol Inflamm* 2022;30(4):973-977.

42 Randon M, Liang H, El Hamdaoui M, *et al*. *In vivo* confocal microscopy as a novel and reliable tool for the diagnosis of *Demodex* eyelid infestation. *Br J Ophthalmol* 2015;99(3):336-341.

43 Wang K, Chen X, He C, *et al*. Information entropy-based framework for quantifying curve tortuosity in meibomian glands uneven atrophy. *Transl Vis Sci Technol* 2026;15(5):25.

44 Wang MJ, Chen XY, Wang KS, *et al*. A new digital biomarker of *Demodex* blepharitis: energy curve of the meibomian edge. *Front Cell Dev Biol* 2025;13:1627327.